IOP Publishing Physica Scripta
Phys. Scr. 95 (2020) 035003 (14pp) https://doi.org/10.1088/1402-4896/ab4939

Dynamics of localized continuum inside a charged particle

S Bhattacharya

Department of Mechanical Engineering, Texas Tech University, Lubbock, TX 79409, United States of America

E-mail: s.bhattacharya@ttu.edu

Received 2 April 2019, revised 15 September 2019
Accepted for publication 30 September 2019
Published 5 February 2020

Abstract

This article explains how a charged body can retain its integrity despite electrostatic repulsion within itself. The study requires derivation of the field equations governing the velocity of any arbitrary element within the system. These relations are obtained from two Lagrangian principles based on obvious and least disruptive modifications of known concepts in classical mechanics. The two Lagrangians lead to a relativistic energy-momentum equation describing the motion and Maxwell's equations quantifying the electromagnetic fields, respectively. The energy-momentum relation shows that rigid body motions creating stationary fields in a rotating frame is a viable solution for the velocity inside the continuum. It also yields a combined potential which remains constant throughout the rotating particle. This constancy coupled with Maxwell's equations and boundary conditions for proper interfacial continuity provides the charge distribution and geometric shape required for continued coherence of the domain. The paper presents specific simulations for slender annuli steadily rotating about the axis of symmetry where the charge density and the axial width are plotted as radial functions. Curiously, when the analysis is extended to systems with different axes of rotation and symmetry, the proportionalities between energy and frequency as well as momentum and wave-number can be established. Such results are very similar to Planck's and de Broglie's laws, even though derived from classical principles. Thus, the presented theory might have deeper implications like, for example, in mathematical computation of fine structure constant.

Keywords: relativistic continuum dynamics, Lagrangian mechanics, vorticity theorem, elementary particles, quantum mechanics fundamentals

1. Introduction

Stable existence of a particle with extremely localized charge is counter-intuitive. If it contains similar charge everywhere, electrostatic repulsion within itself is expected to cause eventual disintegration. In contrast, if opposing charges occupy the volume, a sufficiently large external field can fragment the system. This issue of coherence is explained for atomic nucleus by theorizing the restoring effect of strong force counteracting electrodynamic fields. Strong force is, however, not relevant for elementary particles like electrons or positrons. Hence, it is not obvious how such a charged body can maintain its integrity despite inherent electrostatic repulsions. We attempt to answer this vexing question here by identifying the charged domains capable of retaining their geometry and by analyzing the dynamics inside their interior.

Quantum electrodynamics [1] disregards the aforementioned issue due to axiomatic presumption of point charges. Around the time of quantum revolution, however, there had been numerous classical studies searching for an explanation behind stable dynamics of particles with localized charge [2–4]. Research on related topics has continued for nearly a century, and a number of relevant articles have been published throughout this period [5–10]. Most of these papers have assumed simplistic geometries where configurational coherence requires substantial extrapolation of the known principles of mechanics unfortunately. This is why such analysis necessitates inclusion of stabilizing influence of rather contrived phenomenon like Poincare stresses [11] or gravity-like potentials [12, 13]. The present article demonstrates that a much less disruptive continuum formulation can indeed explain integrity of a charge domain if undue

adherence to presumed geometric models is relaxed. The resulting freedom also allows us to conceive systems with inherent quantum features which can be viewed as potentially the most significant inference drawn from our findings. Consequently, this may eventually lead to a new paradigm where classical interpretation of quantum wave-function and causal explanation of entanglement will be possible.

The key consideration in continuum approach is the finiteness of the volume for any charged matter even if it is very small. The complete dynamics of such a body can only be described by studying the motion of any arbitrary volume element inside the continuum. This formulation is intrinsically different from typical electrodynamic problems, where generally available initial conditions provide starting values of the relevant fields. In contrast, the present analysis assumes no initial condition—it replaces this crucially required information by a criterion for sustained integrity. A sufficient constraint for continued coherence of the material domain is that every material element inside the particle comes back to its original position relative to the center of the body. Thus, this strictly periodic time-dependence in displacement with respect to the center is used to complete the proper mathematical description of the system.

Accordingly, we first investigate whether the well-known principles of classical relativistic mechanics are suitable for addressing the outlined problem. Consequently, an obvious and least disruptive modification in classical continuum equations is proposed, and significant generic features of the corresponding field solutions are identified. Our analysis combines these conclusions with constraints of continuity between electromagnetic fields inside and outside the matter. This ultimately determines the geometries and appropriate charge distribution in the interior of the domain where its continued integrity is ensured by the balance between inertial and electromagnetic force. To demonstrate the practicality of this procedure, we present simulation results that reveal the charge density and the axial width of slender charged annuli steadily rotating about their axis of symmetry. Such approach, when extended to systems with misaligned axes of symmetry and rotation, can establish proportionalities between frequency and energy as well as wave-number and momentum. If these results are linked with Planck's and de Broglie's law, a framework can be built to mathematically compute fine structure constant. The discussed outcomes show validity and potentially significant impact of the constructed theory.

This paper is organized in the following way. In section 2, we find the governing relations from appropriate Lagrangians after minimal tinkering of classical mechanics principles. Section 3 outlines two crucial features of the general solutions for the obtained field equations. Section 4 reveals a steady rigid body rotation as a viable motion for which constancy of a scalar field named as 'combined potential' can be established. In section 5, constancy of the scalar is used in a simplified special problem to simulate the charge density and the axial width of steadily rotating slender annuli as radial functions. Section 6 addresses the general rigid body motion again to derive energy-frequency and momentum-wavelength relations similar to Planck's and de Broglie's laws by extending the analysis to systems with misaligned axes of rotation and geometric symmetry. Finally, the article is summarized, and conclusions are drawn in section 7.

2. Review and reconstruction of classical continuum mechanics

According to classical relativistic continuum mechanics, the energy-momentum conservation relations along with Maxwell's equations govern the fields relevant to dynamics inside a charged body. In this section, we review these field equations starting from basic Lagrangian constructions. The analysis adhere to a doctrine of least disruption so that well-known classical Lagrangian descriptions are altered minimally. The challenge is to see whether such approach can conform to the constraint of sustained integrity requiring strictly periodic unsteadiness in displacements inside the charged domain.

It is to be noted here that even if our least disruptive approach can assure sustained integrity, further tinkering in the Lagrangian formulation might be needed for problems with different length and time scales. For example, an astronomic problem might need modifications in Lagrangians by small corrections which are irrelevant to the system analyzed in the present paper. We, however, keep these questions open for future considerations while focusing on the simplest possible explanations.

2.1. Charged continuum and relevant fields

The mechanics of continuum describes time-dependent motion of each elementary part inside a material domain. Thus, to analyze such dynamics, one has to first form a precise idea about matter and motion.

Our theory considers matter to be identified by its charge content which remains fixed for a specific material volume even if it undergoes arbitrary deformation in the course of its motion. This charge itself might even be zero, but then its absence is the marker for that specific element. If this is considered as an axiomatic statement derived from the conservation of charge, then there is no *a priori* necessity to define mass. In that case, a quantity similar to mass appears subsequently as a consequence of the Lagrangian construction satisfying all relevant properties demanded by classical mechanics.

The motion of a material element is described by the tangent to its trajectory traced in four dimensional (4D) physical space as conceived by special theory of relativity. Accordingly, the 4D space is hyperbolic between time and space, where three dimensional (3D) spatial subspace is elliptic. In absence of an external force field, a convenient description can be offered by a notation where $\vec{\mathbf{b}}$ is interpreted as a 4D vector related to a temporal component b_0 and spatial components represented by $\mathbf{b}$

$$\vec{\mathbf{b}} \longrightarrow \{b_0, \mathbf{b}\}. \tag{1}$$

The hyperbolic nature of the metric coefficients means

$$\vec{\mathbf{b}} \cdot \vec{\mathbf{b}} = b_0^2 - \mathbf{b} \cdot \mathbf{b} = b_0^2 - b_1^2 - b_2^2 - b_3^2 \tag{2}$$

with b_1, b_2, b_3 being three orthonormal spatial components. The conciseness in the expressions and the convenience in switching from 4D to 3D space are the reasons behind our preference for the vector notation involving $\vec{\mathbf{b}}$ and $\mathbf{b}$ instead of the usual covariant representations.

In our mathematical analysis, the 4D position vector $\vec{\mathbf{x}}$ is considered as the only independent variable:

$$\vec{\mathbf{x}} \longrightarrow \{ct, \mathbf{x}\}, \tag{3}$$

where t is time, c is the velocity of light, and $\mathbf{x}$ is the spatial position vector. The gradient in $\vec{\mathbf{x}}$ is given by $\vec{\nabla}$

$$\vec{\nabla} \longrightarrow \left\{ \frac{1}{c}\frac{\partial}{\partial t}, \nabla \right\}, \tag{4}$$

with ∇ representing the spatial derivatives. Also, the motion defining tangent vector $\vec{\mathbf{s}}$ to the trajectory in 4D space is treated as the dependent variable to be evaluated

$$\vec{\mathbf{s}} \longrightarrow \{s_0, \mathbf{s}\} = \left\{ \frac{-c}{\sqrt{c^2 - \mathbf{v} \cdot \mathbf{v}}}, \frac{\mathbf{v}}{\sqrt{c^2 - \mathbf{v} \cdot \mathbf{v}}} \right\}, \tag{5}$$

where $\mathbf{v}$ is rate of change of $\mathbf{x}$ with respect to t as known in Newtonian kinematics.

The conservation of charge ensured by our definition of matter can be given by the following continuity equation

$$\frac{\partial \rho}{\partial t} + \nabla \cdot (\rho\, \mathbf{v}) = -\vec{\nabla} \cdot (\tilde{\rho}\, \vec{\mathbf{s}}) = -\vec{\nabla} \cdot \vec{\mathbf{j}} = 0, \tag{6}$$

where ρ is the charge per unit material volume seen by a stationary observer. In contrast, $\tilde{\rho} = \rho\sqrt{c^2 - \mathbf{v} \cdot \mathbf{v}}$ is the charge density measured by an observer moving with the element where the effect of length contraction is included. The electric current in 4D space is $\vec{\mathbf{j}}$

$$\vec{\mathbf{j}} = \tilde{\rho}\, \vec{\mathbf{s}} \longrightarrow \{-\rho c, \rho \mathbf{v}\}, \tag{7}$$

which has causal relation with all electrodynamic interactions. Its effects on neighboring matter are felt by a 4D vector $\vec{\mathbf{a}} \longrightarrow \{a_0, \mathbf{a}\}$, where $a_0 = -\phi/c$ is related to the electric scalar potential ϕ, and $\mathbf{a}$ is the magnetic vector potential. The main goal of the continuum analysis is to find coupled variables $\vec{\mathbf{j}}$ and $\vec{\mathbf{a}}$ as functions of $\vec{\mathbf{x}}$.

2.2. Lagrangian construction of field equations

The field equations governing $\vec{\mathbf{j}}(\vec{\mathbf{x}})$ and $\vec{\mathbf{a}}(\vec{\mathbf{x}})$ can be derived by using two Lagrangian principles. This is a standard procedure in classical mechanics [14] from which the specific expressions of Lagrangians are imported after a slight modification in the interpretation.

The first Lagrangian principle states that for a known $\vec{\mathbf{a}}(\vec{\mathbf{x}})$ every material element follows a 4D trajectory joining two given points in such a way that the Lagrangian $L_m = \vec{\mathbf{s}} \cdot \vec{\mathbf{a}}$ is extremized among all possible paths. In other words, $\vec{\mathbf{s}}$ is chosen in such a way that L_m is extremized when $\vec{\mathbf{a}}(\vec{\mathbf{x}})$ and two end points on the locus are provided. The statement has a slight departure from traditional classical mechanics where an additional term associated with the mass and the kinetic energy exists in the Lagrangian expression. We, however, note that the same term can be incorporated in the formulation by recognizing the inherent definitional constraint for $\vec{\mathbf{s}}$

$$\vec{\mathbf{s}} \cdot \vec{\mathbf{s}} = 1. \tag{8}$$

Thus, the extremization of L_m in presence of the above condition (equation (8)) implies the following variational relation, where an appropriate Lagrange multiplier ζ is introduced

$$\delta \int_{p_1}^{p_2} (\vec{\mathbf{s}} \cdot \vec{\mathbf{a}} + \zeta \vec{\mathbf{s}} \cdot \vec{\mathbf{s}}) \mathrm{d}C = 0. \tag{9}$$

Here, the integral is over the 4D curve with an elementary curve-length dC in a trajectory connecting any given starting and ending points p_1 and p_2. Also, the scalar field ζ acts as a Lagrange multiplier for the constraint in equation (8). At the same time, it plays the role similar to inertia in the continuum dynamics. Ultimately, the variational principle leads to an energy-momentum field equation

$$-\vec{\mathbf{s}} \cdot \vec{\nabla}(\zeta \vec{\mathbf{s}}) = \vec{\mathbf{s}} \cdot \vec{\nabla}\vec{\mathbf{a}} - (\vec{\nabla}\vec{\mathbf{a}}) \cdot \vec{\mathbf{s}}. \tag{10}$$

It coincides with macroscopic classical electrodynamics, if the Lagrange multiplier ζ is interpreted as mc/q, where m and q are total mass and charge of the particle. In that case, one recovers the well-known relation, where left hand side of equation (10) is rate of change of energy and momentum, while its right hand side is the electrodynamic work and Lorentz force. We are, however, a little reluctant to assert $\zeta = mc/q$, though we concur with the energy-momentum interpretation of equation (10). The reason behind this subtle disagreement is the fact that ζ is a field variable, whereas both m and q are integral quantities associated to the whole system. Hence, in our view, it is premature to relate ζ to m and q at this point—for now ζ should be treated as a Lagrange multiplier and a dependent variable to be determined, nothing more, nothing less. Physically, it dictates how much curvature can be created in 4D locus of an element by the force acting on it. In principle, ζ can even have a sign opposite to the local charge making the so called 'bare mass-density' $\zeta^*\rho < 0$ in the rigion a locally negative quantity. The resulting freedom is crucial as it might be useful in finding a criterion for stability of the system under external or stochastic perturbation. For charged bodies, apparently unrealistic $\zeta^*\rho < 0$ does not necessarily mean unphysical negative inertia for the overall body. Even when $\zeta^*\rho < 0$, added mass due to the electromagnetic field combines with the contribution from the matter to make the particle-inertia positive ensuring no contradiction with all known aspects of observable dynamics.

Unlike the first Lagrangian principle, the second one is a direct implant from classical electrodynamics. It states that for a given $\vec{\mathbf{j}}$, the vector $\vec{\mathbf{a}}$ is such that integral of another Lagrangian denoted by L_f over the 4D volume is extremized. The expression for L_f is known:

$$L_f = \frac{1}{4}[\vec{\nabla}\vec{\mathbf{a}} - (\vec{\nabla}\vec{\mathbf{a}})^T] : [\vec{\nabla}\vec{\mathbf{a}} - (\vec{\nabla}\vec{\mathbf{a}})^T] - \mu_0 \vec{\mathbf{j}} \cdot \vec{\mathbf{a}}, \tag{11}$$

where μ_0 is the magnetic permeability, and the superscript T

indicates transpose of the second order tensor in 4D space. The field equation obtained from equation (11) is

$$\vec{\nabla} \cdot [\vec{\nabla}\vec{\mathbf{a}} - (\vec{\nabla}\vec{\mathbf{a}})^T] = \mu_0 \vec{\mathbf{j}}. \tag{12}$$

This is a condensed and convenient form of Maxwell's relations when $a_0 = -\phi/c$ and $\mathbf{a}$ are considered as the scalar and vector potentials [15].

We solve for ζ, ρ, $\vec{\mathbf{s}}$ and $\vec{\mathbf{a}}$ from equations (10) and (12) which can also be expressed by covariant representations. Both relations are invariant to Lorentz gauge transformation as expected. The related scalar gauge field plays a crucial role in our subsequent analysis.

2.3. Boundary conditions for interfacial continuity

The second order of equation (10) requires two boundary conditions for $\vec{\mathbf{a}}$. Firstly, the exterior fields far away from the particle must decay to zero. Secondly, there cannot be any singularity in the interior of the charged domain.

The system also requires proper continuity at the interface between the interior and the exterior domains. The interfacial discontinuity in $\vec{\mathbf{a}}$ is not permissible, because this means unphysical infinite strength of electromagnetic fields. Moreover, the normal gradient of $\vec{\mathbf{a}}$ must be continuous to ensure finite charge density at the boundary of the particle. These two constraints for continuity help to obtain the geometry of the body and the homogeneous solutions in the mathematical formulations.

For complete mathematical description, the boundary conditions are coupled with the criterion for sustained integrity implied by periodic change in displacement relative to the particle-center. Thus, we intend to identify only these systems instead of finding a general solution.

3. Features of the field solutions

In this section, we identify a few important properties of the general solution for equations (10) and (12). These properties are crucial for finding the solutions which guarantee sustained integrity of the charged particle.

3.1. Lagrange multiplier as constant of motion

We recognize two identities related to the two sides of equation (10). Firstly, if its left hand side is dotted with $\vec{\mathbf{s}}$, the following conclusion can be drawn by applying $\vec{\mathbf{s}} \cdot \vec{\mathbf{s}} = 1$:

$$-\vec{\mathbf{s}} \cdot [\vec{\nabla}(\zeta\vec{\mathbf{s}})] \cdot \vec{\mathbf{s}} = -\vec{\mathbf{s}}.\vec{\nabla}\zeta. \tag{13}$$

Secondly, when the same dot product is performed to the right hand side, the product disappears:

$$[\vec{\mathbf{s}} \cdot \vec{\nabla}\vec{\mathbf{a}} - (\vec{\nabla}\vec{\mathbf{a}}) \cdot \vec{\mathbf{s}}] \cdot \vec{\mathbf{s}} = 0. \tag{14}$$

Thus, combining equations (10), (13) and (14), we can infer

$$\vec{\mathbf{s}}.\vec{\nabla}\zeta = 0. \tag{15}$$

This means that the Lagrange multiplier ζ has to be a constant of motion. The relation is analogous to conservation of rest mass in classical continuum mechanics.

It is to be noted that if a quantity is a constant of motion, it does not necessarily imply its constancy over the entire volume of the particle. From equation (15), we can only infer that ζ is fixed in the course of the motion of an infinitesimally small material element inside the particulate domain. However, ζ can, in general, vary from one element to another. Its invariance over the entire domain can only be attributed from additional considerations.

3.2. Momentum vorticity theorem

When ζ is a constant of motion, the temporal or energy component of equation (10) becomes dependent on its spatial or momentum relations. As a result, the 4D vector equation can only provide three independent relations. Thus, we solely focus on the momentum components of equation (10).

The momentum components of equation (10) describing 3D vector fields in spatial subspace take the following form

$$\frac{\partial}{\partial t}\frac{\zeta\mathbf{v}}{\sqrt{c^2 - v^2}} + \mathbf{v} \cdot \nabla\frac{\zeta\mathbf{v}}{\sqrt{c^2 - v^2}} = (\nabla\mathbf{a}) \cdot \mathbf{v} - \nabla\phi - \frac{\partial\mathbf{a}}{\partial t} - \mathbf{v} \cdot \nabla\mathbf{a}, \tag{16}$$

where $a_0 = -\phi/c$. If momentum $\mathbf{p}$ and energy e per unit charge are defined using known canonical forms

$$\mathbf{p} = \frac{\zeta\mathbf{v}}{\sqrt{c^2 - v^2}} + \mathbf{a}, \qquad e = \frac{\zeta c^2}{\sqrt{c^2 - v^2}} + \phi, \tag{17}$$

one can rewrite equation (16)

$$\frac{\partial\mathbf{p}}{\partial t} + \mathbf{v} \cdot \nabla\mathbf{p} = (\nabla\mathbf{p}) \cdot \mathbf{v} - \nabla e + \sqrt{c^2 - v^2}\,\nabla\zeta. \tag{18}$$

Here, both $\mathbf{p}$ and e are field variables which are functions of space and time. The left hand side of equation (18) is the substantial derivative of momentum per unit charge, whereas the right hand side is force per unit charge.

If the curl of equation (18) is considered, one finds

$$\frac{\mathrm{d}}{\mathrm{d}t}(\nabla \times \mathbf{p}) + (\nabla \times \mathbf{p})\nabla \cdot \mathbf{v} - (\nabla \times \mathbf{p}) \cdot \nabla\mathbf{v} = \nabla\sqrt{c^2 - v^2} \times \nabla\zeta, \tag{19}$$

where $\mathrm{d}/\mathrm{d}t = \partial/\partial t + \mathbf{v} \cdot \nabla$ is the substantial derivative. We recognize the similarity between equation (19) and vorticity transport relation for inviscid fluid [16]. The right hand side of equation (19) acts as a source term akin to baroclinic contribution in variable density fluid, whereas the expression left to the equality represents rate of change of appropriate components of $\nabla \times \mathbf{p}$. The features of equation (19) prompt us to prove a statement analogous to Kelvin's theorem for inviscid flow. Continuum kinematics ensures:

$$\frac{\mathrm{d}}{\mathrm{d}t}(\hat{\mathbf{n}}\delta A) = (\nabla \cdot \mathbf{v})\hat{\mathbf{n}}\,\delta A - (\nabla\mathbf{v}) \cdot \hat{\mathbf{n}}\,\delta A, \tag{20}$$

where $\hat{\mathbf{n}}$ is the unit normal on a material area δA. If equation (19) is dotted with $\hat{\mathbf{n}}\delta A$, and combined with

equation (20), it shows

$$\frac{\mathrm{d}}{\mathrm{d}t}[\hat{\mathbf{n}}\cdot(\nabla\times\mathbf{p})\delta A]=\hat{\mathbf{n}}\cdot(\nabla\sqrt{c^2-v^2}\times\nabla\zeta)\delta A. \quad (21)$$

We refer $\nabla\times\mathbf{p}$ as momentum vorticity and equation (21) as its theorem following the fluid mechanics precedence. This relation implies that if basis vectors remain fixed with a material volume undergoing deformation and rotation, the components of $\nabla\times\mathbf{p}$ in that basis evolve as integrals of the baroclinic term $\nabla\sqrt{c^2-v^2}\times\nabla\zeta$. If $\nabla\sqrt{c^2-v^2}\times\nabla\zeta$ disappears, these components of $\nabla\times\mathbf{p}$ become constants of motion. Here, it is to be noted though that neither the momentum vorticity nor the baroclinic source is an invariant vector in 4D Minkowski space. Thus, even if components of $\nabla\times\mathbf{p}$ in material basis are constant in one reference frame, these can exhibit temporal variations in another. For sake of simplicity, ζ can be heuristically assumed as a constant of space in a special case to avoid potentially distracting mathematical complications. In our subsequent analysis, however, the general system involving radially varying ζ introduces minimal changes. The innocuous nature of the added complexity prompts us to choose generality over simplification.

We recognize the vorticity momentum theorem as a key result useful in determination of the desired field solutions satisfying sustained integrity. Accordingly, the subsequent strategy is going to be a search for a reference frame and a velocity field for which the baroclinic source is automatically $\mathbf{0}$, and material components of $\nabla\times\mathbf{p}$ are obviously constant. Once these general systems are identified, we will focus on a specific special case among these where the appropriate charge densities and the consequent electromagnetic fields will be computed. The purpose of the simulation is to demonstrate viability of the theory in construction of physical solutions associated to a coherent particle with non-zero charge. After establishing such capability, we will revisit the general system to discuss a few important observations which indicate a possible connection between the continuum analysis and the quantum mechanics fundamentals.

4. Rigid body rotation as viable solution for motion

The momentum vorticity theorem equation (21) infers that steady rigid body motion with appropriate charge distribution ensures the satisfaction of all governing equations and boundary conditions. Such motion can be described by a pure rotation about a translating axis. Without an external force, the translation remains time-independent allowing an inertial frame fixed with the axis of revolution. We assume that the entire system is undergoing a rotation without deformation relative to this axis which aligns along the axial coordinate of a cylindrical system. We also consider ζ to vary radially in that cylindrical system. Under the assumed conditions, the baroclinic source in equations (19) and (21) disappears implying $\sqrt{c^2-v^2}\,\nabla\zeta$ a potential vector field. In addition, this makes all fields time-invariant if expressed in terms of rotating co-ordinates and basis vectors. In other words, temporal variations in all fields would appear to an inertial observer only due to the change in rotating co-ordinates and basis vectors in a frame fixed with the particle. It can be proven that equation (21) is then automatically satisfied.

The underlying rationale behind the construction is the obvious fact that $\hat{\mathbf{n}}\cdot\mathbf{q}$ has to be a constant of motion if component of $\mathbf{q}$ with respect to a rotating basis vector like $\hat{\mathbf{n}}$ remains fixed. Thus, equation (21) is immediately satisfied, if components of $\nabla\times\mathbf{p}$ along rotating basis vectors are time-invariant. This observation prompts us to propose rigid body motion as a solution for the velocity field in the system. Moreover, such motion would have an additional appeal by enforcing the condition of periodic deformation needed for sustained integrity. Subsequent analysis first justifies our proposition more clearly, and then outline the details about how to compute the correct charge density in one specific example problem.

4.1. Kinematics of rigid body motion

The relative velocity field with respect to the steadily translating axis of rotation is only due to the rigid body rotation. It can be described by a time-dependent rotation tensor $\mathbf{R}(t)$ which relates initial spatial location $\mathbf{x}_o$ of a material element to its subsequent positions $\mathbf{x}$

$$\mathbf{x}=\mathbf{R}\cdot\mathbf{x}_o. \quad (22)$$

The second order tensor $\mathbf{R}$ in 3D spatial domain is

$$\mathbf{R}(t)=(\mathbf{I}-\hat{\mathbf{e}}\hat{\mathbf{e}})\cos(\Omega)+\mathbf{E}\cdot\hat{\mathbf{e}}\sin(\Omega)+\hat{\mathbf{e}}\hat{\mathbf{e}}. \quad (23)$$

Here, $\mathbf{I}$ and $\mathbf{E}$ are second order identity and third order permutation tensors in 3D. Also, $\hat{\mathbf{e}}(t)$ is time-dependent unit vector representing the instantaneous direction of the axis of rotational displacement, and $\Omega(t)$ is the angle rotated about that line in that specific instant.

A crucial property of $\mathbf{R}$ is that it is orthogonal:

$$\mathbf{R}\cdot\mathbf{R}^T=\mathbf{I}, \qquad \mathbf{R}\times\mathbf{R}^T=\mathbf{R}\cdot\mathbf{E}. \quad (24)$$

This implies

$$\frac{\mathrm{d}}{\mathrm{d}t}(\mathbf{R}\cdot\mathbf{R}^T)=0\Longrightarrow-\frac{\mathrm{d}\mathbf{R}}{\mathrm{d}t}\cdot\mathbf{R}^T=\mathbf{R}\cdot\frac{\mathrm{d}\mathbf{R}^T}{\mathrm{d}t}=\left(\frac{\mathrm{d}\mathbf{R}}{\mathrm{d}t}\cdot\mathbf{R}^T\right)^T \quad (25)$$

making the dot product of the temporal derivative of $\mathbf{R}$ with its transpose an antisymmetric tensor. Any antisymmetric tensor in 3D can be expressed in terms of $\mathbf{E}$

$$\frac{\mathrm{d}\mathbf{R}}{\mathrm{d}t}=-\mathbf{w}\cdot\mathbf{E}\cdot\mathbf{R}=\mathbf{w}\times\mathbf{R}, \quad (26)$$

where $\mathbf{w}(t)$ is a spatially invariant time-dependent vector. Thus, velocity field induced by rotation is given by

$$\mathbf{v}=\frac{\mathrm{d}\mathbf{x}}{\mathrm{d}t}=\frac{\mathrm{d}\mathbf{R}}{\mathrm{d}t}\cdot\mathbf{x}_o=\mathbf{w}\times(\mathbf{R}\cdot\mathbf{x}_o)=\mathbf{w}\times\mathbf{x}. \quad (27)$$

This shows that the description provided by equations (22)–(26) is a concise way to quantify arbitrary unsteady rotation given by Euler. We prefer our tensorial representation for its utility in the subsequent analysis.

4.2. Stationary fields in a rotating frame

A stationary field inside a rigid body is defined by its temporal invariance in a reference frame rotating with the particle. If ψ is a stationary scalar field, it means

$$\psi(t, \mathbf{x}) = \psi(\mathbf{R}^T(t) \cdot \mathbf{x}) = \psi(\mathbf{x}_o), \tag{28}$$

so that it does not vary with time when spatial co-ordinates $\mathbf{x}_o$ attached to the matter are the independent variables. Similarly, if $\mathbf{b}$ is a stationary vector field, a steady vector function $\mathbf{b}_o(\mathbf{x}_o)$ can represent it

$$\mathbf{b}(t, \mathbf{x}) = \mathbf{R}(t) \cdot \mathbf{b}_o(\mathbf{x}_o). \tag{29}$$

Then, components of $\mathbf{b}$ in basis vectors attached to the body remain time invariant if expressed in terms of $\mathbf{x}_o$.

If $\nabla \times \mathbf{p}$ is stationary, momentum vorticity theorem (equation (21)) is obviously satisfied. This is because unit normal $\hat{\mathbf{n}}$ on a material area δA can be treated as a basis vector rotating with the body. Then, temporal invariance of the component of $\nabla \times \mathbf{p}$ along $\hat{\mathbf{n}}$ is assured. In that case, the momentum conservation in equation (18) can be easily satisfied.

Stationary $\nabla \times \mathbf{p}$ implies

$$\mathbf{p}(t, \mathbf{x}) = \mathbf{R} \cdot \mathbf{p}_o(\mathbf{x}_o) + \nabla g. \tag{30}$$

Here, the scalar field g disappears in the expression of $\nabla \times \mathbf{p}$. It is a gauge different than Lorentz's or Coulomb's. The construction in equation (30) is possible when the motion is created by a steady angular velocity ω of a rigid body:

$$\mathbf{w} = \omega \hat{\mathbf{e}} \qquad \Omega(t) = \omega t. \tag{31}$$

The system described in equation (31) is not necessarily time invariant despite constant particulate motion. This dichotomy appears because a steady rotation can still produce unsteady variations to inertial observers [17], if the axis of spin does not coincide with the line of symmetry.

The constraints in equations (27) and (31) are sufficient criteria for sustained integrity ensuring periodic displacement of every material element. Such conditions may not be the necessary ones though. Hence, future research should look for potential generality so that non-rigid deforming systems like in [18] can be viable possibilities.

4.3. Derivation of the combined potential

The satisfaction of equation (19) in a steadily rotating body converts the momentum relation (equation (18)) into a relation where gradient of a scalar function η equates to $\mathbf{0}$ implying constancy of η over the charged continuum. We refer to this spatially invariant scalar function as combined potential whose expression is derived in the subsequent analysis. The final result is analogous to Bernoulli's relation for potential flow in fluid dynamics.

To derive the desired relation, we prove two identities assuming equations (27), (30) and (31) to be true. First of these is

$$\frac{\partial \mathbf{p}}{\partial t} + \mathbf{v} \cdot \nabla \mathbf{p} - (\nabla \mathbf{p}) \cdot \mathbf{v} = \nabla \frac{\partial g}{\partial t} - \mathbf{w} \times \mathbf{p}_s - (\nabla \mathbf{p}_s) \cdot \mathbf{v}, \tag{32}$$

where $\mathbf{p}_s$ is the stationary part of momentum $\mathbf{p}$ in equation (30)

$$\mathbf{p}_s = \mathbf{R} \cdot \mathbf{p}_o(\mathbf{x}_o). \tag{33}$$

The second identity concludes

$$\mathbf{w} \times \mathbf{p}_s = [\nabla(\mathbf{w} \times \mathbf{x})] \cdot \mathbf{p}_s = (\nabla \mathbf{v}) \cdot \mathbf{p}_s. \tag{34}$$

Subsequently, equations (32) and (34) are combined by exploiting product rule of differential to convert equation (18) into a gradient relation indicating irrotationality

$$\nabla \left[\frac{\partial g}{\partial t} + g_\zeta - \mathbf{p}_s \cdot \mathbf{v} + \phi + \frac{\zeta c^2}{\sqrt{c^2 - v^2}} \right] = 0. \tag{35}$$

Here, g_ζ can be obtained from a model for ζ by equating ∇g_ζ to the potential field $\sqrt{c^2 - v^2}\, \nabla \zeta$. As g_ζ disappears for constant ζ, its existence is the only difference between systems with radially varying and spatially invariant ζ.

We identify the combined potential η as

$$\eta = \frac{\partial g}{\partial t} + g_\zeta - \mathbf{p}_s \cdot \mathbf{v} + \phi + \frac{\zeta c^2}{\sqrt{c^2 - v^2}}. \tag{36}$$

Its gradient has to disappear according to equation (35) so that the momentum conservation relation in equation (18) is satisfied. Thus, η remains a constant throughout the charged domain according to equation (35). Such constancy is similar to Bernoulli's equation in inviscid flow, and is a convenient feature for determination of the charge density, the electromagnetic fields and the geometric shape defining the charged particle. We set the value of the constant η to 0, as g has sufficient freedom to be adjusted accordingly.

4.4. Governing equations for the reduced system

The description of the system is simplified when stationary fields inside a steadily rotating charged body are considered. This is caused by decrease in dependent variables, as $\mathbf{v}$ becomes completely known. At the same time, automatic satisfaction of momentum relation (equation (18)) and constraint for particulate coherence reduces the number of governing equations and boundary conditions.

For convenience in analysis, we replace $\mathbf{p}_s$ defined in equation (33) by a similarly stationary vector potential $\mathbf{a}_s$

$$\mathbf{a}_s = \mathbf{p}_s - \frac{\zeta \mathbf{v}}{\sqrt{c^2 - v^2}}. \tag{37}$$

As Maxwell's relations include $\mathbf{a}_s$, we prefer it over $\mathbf{p}_s$.

Thus, the dependent variables in the reduced problem are the stationary vector potential $\mathbf{a}_s$, electric potential ϕ, charge density ρ and gauge function g which should be governed by one vector and three scalar equations. The first of these is provided by the constancy of the combined potential η after

equation (36) is substituted in equation (37)

$$\frac{\partial g}{\partial t} + g_\zeta - \mathbf{a}_s \cdot \mathbf{v} + \phi + \zeta\sqrt{c^2 - v^2} = 0. \tag{38}$$

In addition, Maxwell's relations are

$$\frac{1}{c^2}\frac{\partial^2 \phi}{\partial t^2} - \nabla^2\phi = \mu_0 c^2 \rho, \quad \frac{1}{c^2}\frac{\partial^2 \mathbf{a}_s}{\partial t^2} - \nabla^2 \mathbf{a}_s = \mu_0 \rho \mathbf{v}. \tag{39}$$

Finally, the Lorentz gauge constraint is set:

$$\frac{1}{c^2}\frac{\partial \phi}{\partial t} + \nabla \cdot \mathbf{a}_s = 0, \tag{40}$$

which simplifies equation (39), but necessitates the appearance of g in equation (38). The system can be further reduced by eliminating g and disregarding equation (40). The consequent complexities in equation (39), however, prohibit us to follow that path. Hence, we decide to seek stationary fields that satisfy equations (38)–(40). The resulting formulation provides the appropriate geometry and charge distribution so that the rate of change of momentum field can counterbalance electrodynamic forces sustaining coherence.

5. Simulation of geometries and fields for steadily rotating annuli

The stationary solutions for equations (38)–(40) are easiest to find where an axisymmetric system does not show any temporal variation in either rotating or inertial reference frame. In other words, the geometry has a line of symmetry about which the body rotates with a constant speed ω. In this section, we consider specific examples of such geometry in the form of slender disc-like annuli.

Moreover, we will consider a further simplification where ζ is assumed to be constant throughout the domain. Then, the scalar field g_ζ introduced in equation (35) disappears from the expression of η. This consideration makes the trajectories of different parts of the particle similarly curved due to action of an external force creating a possibility of coherence even under external disturbance.

The purpose of the presented simulation is to show that our formulation can construct systems with sustained integrity despite non-zero net charge under isolated unperturbed condition. As a result, one can compute specific geometries with proper charge distribution where centripetal inertia due to rotational motion exactly balances the electromagnetic force. Thus, we can demonstrate that the described annuli can maintain their coherence obeying classical electrodynamic principles.

5.1. Normalizing scales for non-dimensional fields

The first step in the simulation is to identify proper scales for all variables so that non-dimensional quantities can be defined. The obvious scales for time, length and velocity are given by t_s, l_s and v_s, respectively

$$t_s = 1/\omega, \qquad l_s = c/\omega, \qquad v_s = c. \tag{41}$$

We take l_s to be isotropic, even though slenderness of the body might imply a different characteristic dimension in the axial direction.

The entire domain has a fixed charge q which is used to find the scales for charge density, electric potential and magnetic potential defined as ρ_s, ϕ_s and a_{ss}, respectively:

$$\rho_s = q\omega^3/c^3, \qquad \phi_s = \mu_0 q\omega c, \qquad a_{ss} = \mu_0 q\omega. \tag{42}$$

The scale for current density, if needed, would be $\rho_s c$.

For non-dimensionalization, the dimensional variables are divided by their scales. Accordingly, non-dimensional radial and axial cylindrical co-ordinates are $\bar{r}$ and $\bar{z}$

$$\bar{r} = r/l_s = \omega r/c, \qquad \bar{z} = z/l_s = \omega z/c, \tag{43}$$

where r, z are their dimensional counterparts. Similarly

$$\bar{t} = t/t_s = \omega t, \quad \bar{\rho} = \rho/\rho_s, \quad \bar{\phi} = \phi/\phi_s, \quad \bar{\mathbf{a}}_s = \mathbf{a}_s/a_{ss}, \tag{44}$$

are all relevant dimension-less quantities.

Rigid body rotation with axial symmetry of the considered system suggests the following simplifications

$$\bar{\mathbf{v}} = \mathbf{v}/c = \bar{r}\hat{\mathbf{e}}_\theta \qquad \bar{\mathbf{a}}_s = \bar{a}_\theta \hat{\mathbf{e}}_\theta, \tag{45}$$

where $\hat{\mathbf{e}}_\theta$ is the unit vector in direction of variation of the cylindrical angle. Also, the temporal invariance of the system converts the time derivative of the gauge function g in equation (38) to a constant whereas invariance of ζ ensures $g_\zeta = 0$. Hence, equations (38)–(40) become cold Euler–Maxwell equation, and simplify into three scalar relations:

$$\bar{r}\,\bar{a}_\theta - \bar{\phi} = \bar{\beta}(\sqrt{1 - \bar{r}^2} + \bar{k}_g), \tag{46}$$

$$(1 - \bar{r}^2)\bar{\nabla}^2\bar{\phi} - \frac{2}{\bar{r}}\frac{\partial \bar{\phi}}{\partial \bar{r}} = -\bar{\beta}\bar{r}\frac{\mathrm{d}}{\mathrm{d}\bar{r}}\left(\frac{1}{\bar{r}}\frac{\mathrm{d}}{\mathrm{d}\bar{r}}\sqrt{1 - \bar{r}^2}\right), \tag{47}$$

and

$$\bar{\rho} = -\frac{1}{1 - \bar{r}^2}\left[\frac{2}{\bar{r}}\frac{\partial \bar{\phi}}{\partial \bar{r}} + \frac{\bar{\beta}\bar{r}^2}{(1 - \bar{r}^2)^{3/2}}\right]. \tag{48}$$

Here, $\bar{\nabla}$ represents gradient in non-dimensional spatial co-ordinates, and $\bar{k}_g$ is the non-dimensional gauge constant to be determined by exploiting boundary conditions. Also, $\bar{\beta}$ is a fixed dimension-less parameter:

$$\bar{\beta} = \frac{\zeta}{\mu_0 q\omega}. \tag{49}$$

This should be evaluated by enforcing

$$\int \bar{\rho}\, \mathrm{d}^3\bar{\mathbf{x}} = \pm 1, \tag{50}$$

where the integral is over the dimension-less volume of the entire charged particle. It is equated to ± 1 so that the charge content in the whole body remains $\pm q$.

5.2. Brief outline of the computational procedure

Conveniently, equations (46)–(48) are all linear and steady relations. So, a finite difference scheme with appropriate spatial discretization can find the numerical solutions for $\bar{\rho}$, $\bar{\phi}$ and $\bar{a}_\theta$. Accordingly, these variables are represented in

discretized form by column $|\rho\rangle$, $|\phi\rangle$ and $|a\rangle$, whose elements are the respective values at spatial grids.

We realize that $\bar{\rho}$ and $\bar{\phi}$ are coupled by two independent linear relations. Firstly, $\bar{\rho}$ can be obtained from $\bar{\phi}$ by using equation (48) whose finite difference discretization yields

$$|\rho\rangle = [S]|\phi\rangle + \bar{\beta}|\psi\rangle. \tag{51}$$

Here, the elements of column $|\psi\rangle$ represent the known radial function multiplied to $\bar{\beta}$ in the right hand side of equation (48). In contrast, the square matrix $[S]$ is formed by discrediting the differential operator acting on $\bar{\phi}$ in equation (48). In the second relation, $\bar{\phi}$ is equated to the Biot–Savart integral corresponding to a Poisson's equation $-\bar{\nabla}^2\bar{\phi} = \bar{\rho}$

$$\bar{\phi}(\bar{\mathbf{x}}) = \int \frac{\bar{\rho}(\bar{\mathbf{x}}')\mathrm{d}^3\bar{\mathbf{x}}'}{4\pi|\bar{\mathbf{x}} - \bar{\mathbf{x}}'|} \qquad \Longrightarrow \qquad [B]|\rho\rangle = |\phi\rangle. \tag{52}$$

We explicitly evaluate the square matrix $[B]$ representing the kernel of the Biot–Savart integral in equation (52). If dependent variables $\bar{\rho}$ and $\bar{\phi}$ satisfy both equations (51) and (52), then all boundary conditions including interfacial continuity are automatically enforced.

The first step in a general simulation starts with an initial guess of the system geometry. Then, equations (51) and (52) need to be combined by eliminating $\bar{\phi}$ to find a matrix equation solely involving $\bar{\rho}$

$$[I - SB]|\rho\rangle = \bar{\beta}|\psi\rangle. \tag{53}$$

Next, the charge distribution can be determined from equation (53) by a simple inversion of $[I - SB]$, where $[I]$ is the identity matrix. Subsequently, the computed charge density should be used in equation (51) to find $\bar{\phi}$ which would, in turn, be utilized in equation (46) for calculation of the vector potential $\bar{a}_\theta$. Finally, the shape of the domain as well as the gauge constant $\bar{k}_g$ are modified iteratively to ensure zero charge density at a layer attached to the periphery of the particle.

The initial simulation results obtained by the outlined general procedure allow us to simplify the computation substantially. These findings show the axial thickness of the annuli to be very thin compared to the radial dimensions especially in the region of denser charge. As a result, we can approximate the system as a saucer-like two dimensional geometry with negligible axial variations due to small height. Consequently, an effective surface charge density $\bar{\sigma}$ with predominantly radial variation can describe the dynamics

$$\bar{\sigma} = 2\int_0^{\bar{h}} \bar{\rho}\, \mathrm{d}\bar{z}, \tag{54}$$

where $\bar{h}(\bar{r})$ is the radially varying half-width of the domain along the z direction. One can relate $|\phi\rangle$ and $|a\rangle$ to $\bar{\sigma}$ considering electrodynamic relations as Poisson's equation. Thus, the following matrix relations are available

$$|\phi\rangle = [\tilde{B}]|\sigma\rangle, \qquad |a\rangle = [\tilde{A}]|\sigma\rangle, \tag{55}$$

where elements of the column $|\sigma\rangle$ are the different values of $\bar{\sigma}$ at different radial grid points. The coupling square matrices $[\tilde{B}]$ and $[\tilde{A}]$ are calculated from explicit elliptic integrals derived by integrating the Biot–Savart kernels over angle θ. Hence, $|\sigma\rangle$ is evaluated by exploiting the matrix form of equation (46)

$$[\tilde{R}\tilde{A} - \tilde{B}]|\sigma\rangle = \bar{\beta}|\tilde{\psi}\rangle + \bar{k}_g\rangle, \tag{56}$$

where $[\tilde{R}]$ is a diagonal matrix with radial positions of the grid points as elements, and the column $|\tilde{\psi}\rangle$ represents the $\bar{r}$-dependent term in the right hand side of equation (46).

The system geometry is defined by the axial width $\bar{h}(\bar{r})$ as well as the inner and outer radii $\bar{r}_i$ and $\bar{r}_o$. After finding $|\sigma\rangle$, we iteratively determine $\bar{r}_i$ and $\bar{r}_o$ along with $\bar{k}_g$ enforcing $\bar{\sigma} = 0$ at both $\bar{r} = \bar{r}_i$ and $\bar{r} = \bar{r}_o$. Then, $\bar{\phi}$ and $\bar{a}_\theta$ are computed from equation (55). Also, approximate leading order $\bar{\rho}$ is evaluated by using equation (48). Finally, the axial thickness $\bar{h}(\bar{r})$ is evaluated by dividing $\bar{\sigma}$ by $2\bar{\rho}$.

The outlined method gives a leading order description of the slender system. We also use the general scheme discussed before to capture the axial changes which seem to be negligible variations (less than 1%). Thus, we present the results from the simplified slender body analysis next.

5.3. Evaluation of the radial dimensions

The most challenging component of the simulation is to identify potential geometries which correspond to mathematically valid and physically meaningful radial variations of the evaluated functions. Hence, the first task in the computation is to recognize the allowable region in the parametric space formed by the geometry-defining quantities. In our slender body problem, inner and outer radii $\bar{r}_i$ and $\bar{r}_o$ dictate the basic features of the system. Among these, if one is given, the other can be determined along with the gauge constant $\bar{k}_g$ by enforcing $\bar{\sigma}$ to disappear at the inner and outer edges of the slender disk. Thus, we choose $\bar{r}_i$ independently, and compute $\bar{r}_o$ and $\bar{k}_g$ by satisfying the consistency at the edges.

Our study reveals that an arbitrary value of $\bar{r}_i$ is not permissible for slender body analysis. For physically meaningful systems, $\bar{\sigma}$ and $\bar{\rho}$ should have same sign at every radial position inside the annular domain. Otherwise, the thickness $\bar{h}$ at a certain location would be negative making the geometry physically absurd. We find out that the positive definiteness of $\bar{h}$ is assured if $0.897 < \bar{r}_i$. Also, the numerical errors in the computed elliptic integrals used in calculations of $[\tilde{A}]$ and $[\tilde{B}]$ (equation (55)) increase when $\bar{r}_i > 0.96$. Thus, to ensure less than 1% relative error as well as permissible geometry, we confine our study in a parametric region $0.897 < \bar{r}_i < 0.95$.

In figure 1, we plot the outer radius as a function of $\bar{r}_i$ within the designated range. Two different values of the number of grid points N are chosen as either 500 or 1000. The results demonstrate good numerical convergence and negligible numerical errors. The value of $\bar{r}_o$ varies within a short range very near to unity. This means that the velocity at the outer edge approaches c. We expect this behavior because stability of the rotating charge is possible only when the magnetic effect is strong enough to counter-balance the electrostatic repulsion. This fact can also explain the permissible region for $\bar{r}_i$—the inner radius cannot be too small so

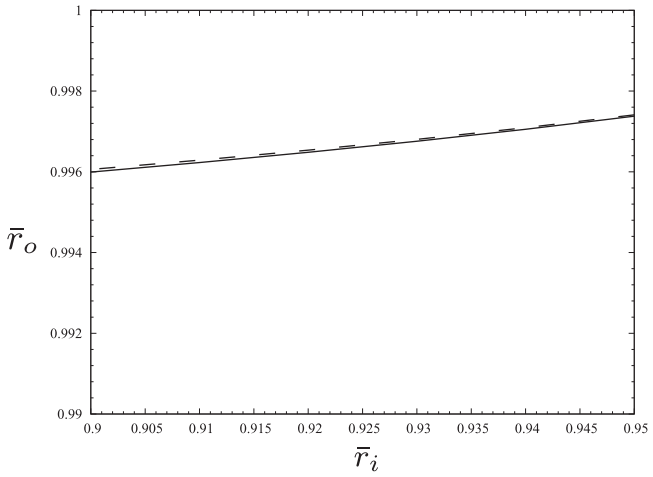

Figure 1. Normalized outer radius corresponding to permissible geometry is presented as a function of normalized inner radius. The simulation is performed for radial grid points $N = 1000$ (solid line) and $N = 500$ (dashed line).

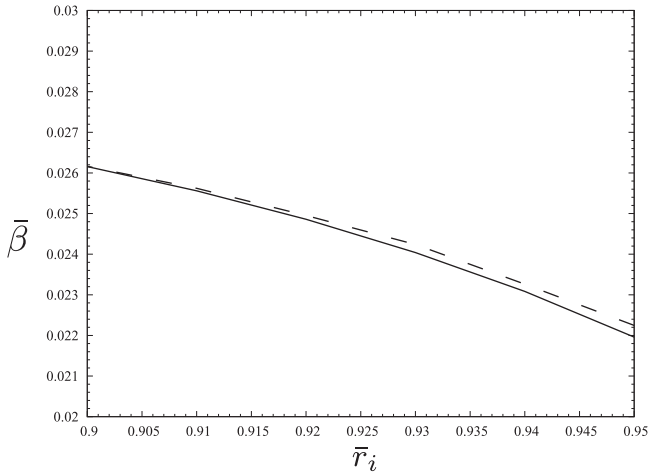

Figure 2. Non-dimensional parameter $\bar{\beta}$ defined in equation (49) is presented as a function of normalized inner radius for radial grid points $N = 1000$ (solid line) and $N = 500$ (dashed line).

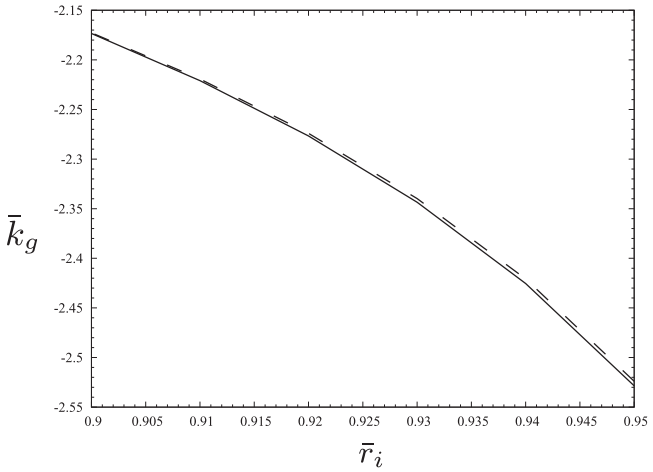

Figure 3. Non-dimensional gauge constant $\bar{k}_g$ is presented as a function of normalized inner radius for radial grid points $N = 1000$ (solid line) and $N = 500$ (dashed line).

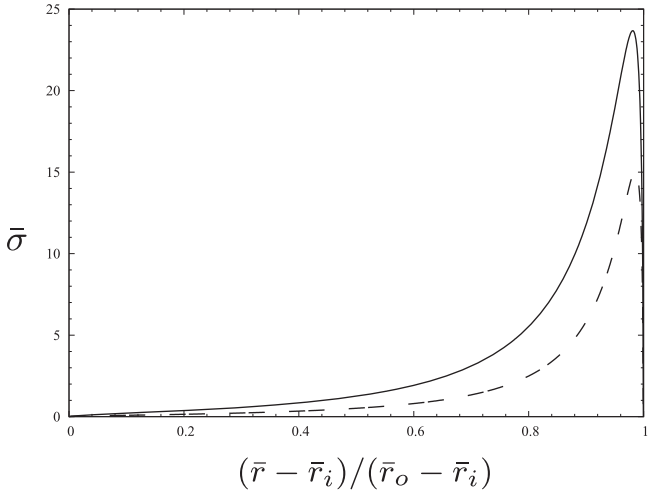

Figure 4. Dimension-less surface charge density $\bar{\sigma}$ versus relative radial position between the inner and outer radius for $\bar{r}_i = 0.95$ (solid line) and $\bar{r}_i = 0.9$ (dashed line).

that the magnetic field becomes negligible near the interior edge.

In figure 2, convergence of gauge constant $\bar{k}_g$ with N is presented for systems with different $\bar{r}_i$. Similarly, figure 3 shows the same for the parameter $\bar{\beta}$ in equation (50). Both reveal good convergence indicating small numerical errors.

5.4. Surface charge distribution and field quantities

The computation method outlined earlier is used to compute the surface charge density $\bar{\rho}$ next. Accordingly, equation (56) is inverted to find $|\sigma\rangle$ from which the values for each radial grid point are evaluated. This result is presented in figure 4, where the radial position is recalibrated so that the transformed variable is 0 at $\bar{r} = \bar{r}_i$ and 1 at $\bar{r} = \bar{r}_o$. The plots show that $\bar{\sigma}$ is small near the inner periphery of the annular domain. Then, the function increases rapidly with increasing radius. Such behavior ensures a positive radial gradient in the electric potential so that the inward electrostatic force hold the inside core together by providing the required centripetal acceleration necessary for the rotational motion. However, the charge density starts to decay fast after attaining a maximum very near to the outer edge. At this point, both the magnetic and electric potentials start to decrease, but the former has a stronger variation. Hence, the magnetic effect not only compensates the outward electric force near the external periphery but also can create enough inward force needed for the motion.

The discussed nuances are further explained by the radial variations in electric potential $\bar{\phi}$ and magnetic potential $\bar{a}_\theta$. We plot $\bar{\phi}$ and $\bar{a}_\theta$ as functions of radial position in figures 5 and 6, respectively. These quantities have their maximum values near the outer edge. One can see subtle differences in two sides of this region of maximization. In the segment with positive radial gradient, electric effect is dominant over magnetic influence causing radially inward net force. In contrast, the situation reverses in the other side of the

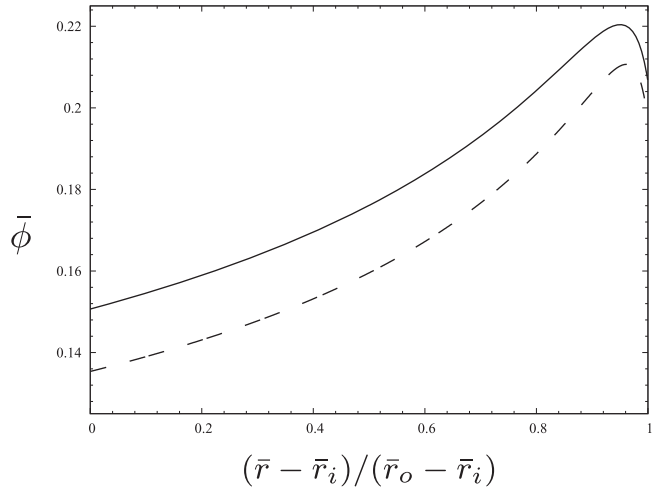

Figure 5. Normalized electric potential $\bar{\phi}$ versus radial position for $\bar{r}_i = 0.95$ (solid line) and $\bar{r}_i = 0.9$ (dashed line).

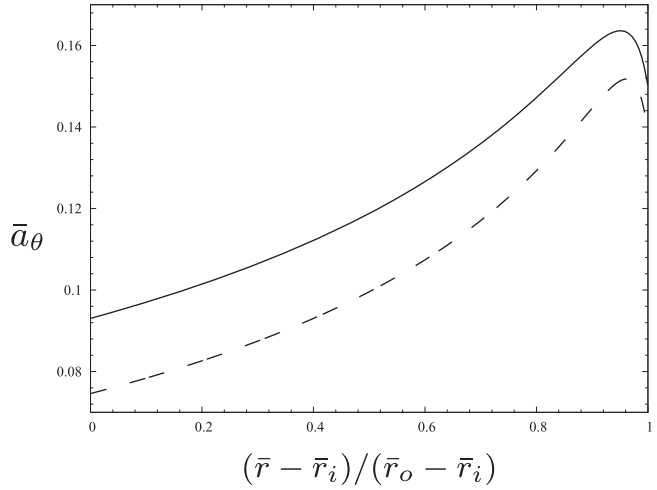

Figure 6. Normalized magnetic vector potential $\bar{a}_\theta$ versus radial position for $\bar{r}_i = 0.95$ (solid line) and $\bar{r}_i = 0.9$ (dashed line).

maxima, because $\bar{a}_\theta$ has a relatively sharper decline than $\bar{\phi}$. As a result, the net electromagnetic force is again radially inward, and the required centripetal acceleration is supplied for the rotational motion.

In figures 4–6, the results are plotted for two systems. First of these is the narrower band where $\bar{r}_i$ is 0.95, and the corresponding $\bar{r}_o$ from figure 1 is 0.997 3775. In contrast, the second is near the critical geometry with $\bar{r}_i = 0.9$ which is near the least permissible value 0.897. One can see $\bar{\sigma}$ is higher in the former. This is because smaller radial span requires larger density to make net charge same as given by equation (50). This, consequently, causes higher $\bar{\phi}$ and $\bar{a}_\theta$ in the narrower domain.

It is to be noted that the velocity approaches to c near the outer rim of the annuli. This does not, however, make the obtained solution invalid, as all the results in this fully relativistic formulation are derived from equations (10) and (12) which have complete covariant representation in hyperbolic Minkowski space. Hence, equation (46) and its corresponding matrix representation equation (56) ensure a perfect balance

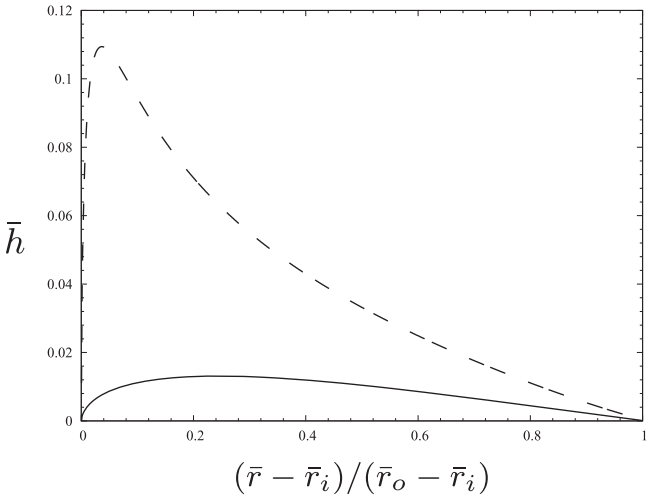

Figure 7. Normalized magnetic vector potential $\bar{a}_\theta$ versus relative radial position between the inner and outer radius for $\bar{r}_i = 0.95$ (solid line) and $\bar{r}_i = 0.9$ (dashed line).

among electric, magnetic and inertial forces throughout the entire material domain from the core to the rim. We recheck this fact by dividing the difference between electric and magnetic forces by the inertial contribution. The resulting ratio is uniformly 1 for the entire radial span $\bar{r}_i \leqslant \bar{r} \leqslant \bar{r}_o$.

5.5. Determination of the radial variation in width

The final task of the simulation is to determine the axial dimension of the annular domain as a radial function, and check whether it conforms with our slender body presumption. For such geometries, the half width $\bar{h}$ for the annulus is calculated by

$$\bar{h} = \bar{\sigma}/(2\bar{\rho}), \tag{57}$$

where volumetric charge density $\bar{\rho}$ is given by equation (48). This construction automatically satisfies the continuity between leading order axial gradient of electrodynamic quantities inside and outside of the charged particle. As a result, radial variation of $\bar{h}$ presented in figure 7 completes the description of the system under consideration.

Volumetric charge density increases sharply with radius according to equation (48). As this change over-compensates the variation in $\bar{\sigma}$, one expects $\bar{h}$ to be a decaying radial function near the outer edge. Also, $\bar{h} = 0$ at $\bar{r} = \bar{r}_i, \bar{r}_o$, because $\bar{\sigma}$ is set to be 0 at the edges in our construction. These features are evident in figure 7.

One can also see distinct differences in the shape of the two domains shown in figure 7. The axial thickness is much smaller for narrower radial band with $\bar{r}_i = 0.95$. In contrast, as $\bar{r}_i$ approaches its critical value of 0.897, the body widens in z direction near the inner edge. Actually, if $\bar{r}_i = 0.897$, then $\bar{h}$ at $\bar{r} = \bar{r}_i$ is infinity, as $\bar{\rho}$ is 0 there. For even smaller inner radius, $\bar{\rho}$ is negative making the width negative in turn after a certain interior point. This is the basic reason for critical nature of the value 0.897 for $\bar{r}_i$. The increase in axial thickness near the inner edge is a simple manifestation of this critical feature.

6. Momentum-wavenumber and energy-frequency proportionalities

It is possible to construct a number of systems with specific geometries and charge densities for which the isolated particle can maintain its self-sustaining coherence. In these material domains, electro-magnetic fields ensure the exact balance between the net force and the required centripetal inertia for rigid body rotation as seen in the previous section. The steady dynamics described in the earlier section shows only a few examples of such systems. The important question is how to characterize the crucial aspects of the dynamics for all possible solutions.

Hence, our main goal in this section is to highlight any major general feature of the possible systems with sustained integrity. Among the charged particles undergoing rigid body rotation, one can conceive a situation where the system steadily rotates about an axis which is not its axis of symmetry. This represents an intrinsically different dynamics than the one seen in the previous section, because when axes of symmetry and rotation do not coincide, wave-like unsteadiness is manifested to an inertial observer even for steady particulate motion. The present section focuses on analyzing such time-dependent behavior in the electrodynamic fields produced by the asymmetrically rotating charged bodies with variable ζ.

The perceived model is slightly different than the accepted description of elementary charge particles which are typically assumed to have axial symmetry. In contrast, we propose a rotating stationary configuration which may have possible azimuthal variations. This apparent contradiction is, however, easily explainable if one considers very fast revolving geometry which would make the system appear as an axisymmetric one for an observation time-scale much larger compared to the period of rotation. As a result, any manifestation of electric or magnetic multipoles would reveal as axisymmetric to a macroscopic observer. Thus, the postulated dynamics can conform to well-known observations despite a fundamental conceptual departure in short-time behavior.

It is to be noted that the stable existence of all these systems depends on whether their integrity can be maintained even under the action of an external force field. The stability criteria in non-dissipative systems as outlined in [19] under different externally imposed perturbations should be a topic of future research. At this point, we are, however, not interested in identifying all possible stable and unstable solutions, as it requires understanding many-body interactions. We concentrate, instead, on the general temporal variations shown by an isolated particle in an inertial frame of reference.

6.1. Transformations from inertial to rotating frames

The temporal derivatives in inertial co-ordinates and in the ones rotating with the rigid body are related:

$$\frac{\partial}{\partial t}_{|\mathbf{x}} = \frac{\partial}{\partial t}_{|\mathbf{x}_o} - (\mathbf{w}\times\mathbf{x}_o)\cdot\nabla_o. \tag{58}$$

Here, initial and later positions $\mathbf{x}_o$ and $\mathbf{x}$ are related by equation (22), whereas ∇_o is the gradient in $\mathbf{x}_o$. We derive equation (58) by using properties in equation (24) and the fact that angular velocity $\mathbf{w}$ is an eigen vector of rotation tensor $\mathbf{R}$

$$\mathbf{R}\cdot\mathbf{w} = \mathbf{w}. \tag{59}$$

If the axes of symmetry and rotation coincide, we find

$$(\mathbf{w}\times\mathbf{x}_o)\cdot\nabla_o = 0, \tag{60}$$

making the two temporal derivatives in two different reference frames given in equation (58) exactly the same.

Temporal variations in any stationary scalar ψ or vector $\mathbf{b}$ are given below, when these satisfy equations (28) and (29):

$$\begin{aligned}\frac{\partial\psi}{\partial t}_{|\mathbf{x}} &= -(\mathbf{w}\times\mathbf{x}_o)\cdot\nabla_o\psi,\\ \frac{\partial\mathbf{b}}{\partial t}_{|\mathbf{x}} &= (\mathbf{w}\times+\mathbf{w}\cdot\mathbf{E}\colon\mathbf{x}_o\nabla_o)\mathbf{R}\cdot\mathbf{b}_o.\end{aligned} \tag{61}$$

Such dependence on time ensures that if the rotating coordinates and basis vectors are chosen, ψ and components of $\mathbf{b}$ become temporally invariant.

If we consider that scalars g, ϕ, ρ and vectors $\mathbf{v}$, $\mathbf{a}_s$ are all stationary in rotating frame like ψ and $\mathbf{b}$, equations (38)–(40) transform into the following forms

$$-(\mathbf{w}\times\mathbf{x}_o)\cdot(\mathbf{a}_o+\nabla_o g)+g_\zeta+\phi+\zeta\sqrt{c^2-v^2}=0, \tag{62}$$

$$\left[\frac{1}{c}(\mathbf{w}\times\mathbf{x}_o)\cdot\nabla_o\right]^2\phi-\nabla_o^2\phi=\mu_0c^2\rho, \tag{63}$$

$$\begin{aligned}&\mathbf{w}\times(\mathbf{w}\times\mathbf{a}_o)+\{(\mathbf{w}\times\mathbf{x}_o)\cdot\nabla_o\}^2\mathbf{a}_o-2(\mathbf{w}\times\mathbf{x}_o)\\ &\cdot\nabla_o\mathbf{w}\times\mathbf{a}_o-c^2\nabla_o^2\mathbf{a}_o=\mu_0c^2\rho\mathbf{w}\times\mathbf{x}_o,\end{aligned} \tag{64}$$

and

$$-\frac{1}{c^2}(\mathbf{w}\times\mathbf{x}_o)\cdot\nabla_o\phi+\nabla_o\cdot\mathbf{a}_o=0, \tag{65}$$

with $\mathbf{a}_o$ being the $\mathbf{x}_o$-dependent factor in $\mathbf{a}_s$. We use the equalities in equation (61) to derive equation (62) from constancy of combined potential, equations (63)–(64) from Maxwell's relations, and equation (65) from Lorentz gauge constraint.

The key feature in equations (62)–(65) is that these are all time-independent relations like equations (46)–(48). Consequently, all dependent fields g, ρ, ϕ, $\mathbf{a}_o$ vary as functions of the rotating spatial co-ordinates $\mathbf{x}_o$ only. In other words, when expressed in terms of $\mathbf{x}_o$, dependent variables g, ρ, ϕ, $\mathbf{a}_o$ are temporally invariant, and their solutions are stationary scalar and vector fields given by equations (28) and (29). Such temporal invariance is expected because both the energy-momentum and electrodynamic equations retain their forms under rotational transformations.

Thus, if a certain class of geometry is considered for an asymmetrically rotating steady rigid body motion, the simulation presented in the previous section can also be extended to solve equations (62)–(65). Consequently, the geometry as well as the charge distribution for the new systems can be computed ensuring continued integrity like before. The only difference in the two problems would be in the details—for

example, the elliptic integrals that construct the square matrices would be formed considering retarded potential instead of Coulombic interactions used earlier. This enables explorations of different kinds of charged domains with sustained coherence. In all cases, satisfaction of equations (62)–(65) ensures such multipolar contributions [20] that the surface integral of Poynting's vector at infinity disappears making the electromagnetic radiation zero despite inherent variations in time.

6.2. Energy and momentum in an inertial reference

At this point, let us assume that an asymmetrically rotating charged domain with sustained coherence has been identified, where all relevant fields and the geometry are known. We intend to find the energy and momentum of the entire system measured by an inertial observer.

At first, we consider an inertial observer who is translating with the axis of rotation. The total linear momentum $\mathbf{p}_{\rm sys}$ of the system in the conceived reference frame is $\mathbf{0}$. The total energy $e_{\rm sys}$ for that charged body does not, however, disappear because different parts of the localized continuum move and experience electro-magnetic interactions. One can calculate $e_{\rm sys}$ as:

$$e_{\rm sys} = \frac{\mu_0 q^2 c}{4\pi\bar{\alpha}}\,\omega, \tag{66}$$

where $\bar{\alpha}$ is a non-dimensional integral given in terms of known non-dimensional field quantities:

$$\frac{1}{\bar{\alpha}} = 4\pi \int\left(\bar{\phi} + \bar{r}\bar{a}_\theta + \frac{\bar{\beta}}{\sqrt{1-\bar{r}^2}}\right)\bar{\rho}\,\mathrm{d}^3\mathbf{x}_o. \tag{67}$$

Here, non-dimensional variables $\bar{r}$, $\bar{\rho}$, $\bar{\phi}$, $\bar{a}_\theta$ are normalized according to equations (43) and (44) by the scales defined in equations (41) and (42). Dimension-less constant $\bar{\beta}$ is obtained using charge normalization in equation (50). As the fields are steady when expressed in terms of $\mathbf{x}_o$, the integral representing $\bar{\alpha}$ does not change with time. We refer to $\bar{\alpha}$ as the structure constant which remains unique for a specific coherent system. For the symmetrically rotating annuli, $1/\bar{\alpha}$ is 14.63 and 13.96 for $\bar{r}_i = 0.95$ and $\bar{r}_i = 0.9$, respectively. If the geometry and charge distribution for particles like electron or positron are identified, the value of $\bar{\alpha}$ should coincide with the fine structure constant. We believe that such systems must rotate asymmetrically exhibiting temporal variations to an inertial observer.

When an observer moves relative to the axis of rotation with a translational velocity $-\mathbf{u}$, the new energy $\tilde{e}_{\rm sys}$ and momentum $\tilde{\mathbf{p}}_{\rm sys}$ of the system satisfy Lorentz transformation. The new values $\tilde{e}_{\rm sys}$ and $\tilde{\mathbf{p}}_{\rm sys}$ in the new frame are related to the old values $e_{\rm sys}$ and $\mathbf{p}_{\rm sys}$ by

$$\tilde{e}_{\rm sys} = \frac{e_{\rm sys}}{\sqrt{1-u^2/c^2}}, \tag{68}$$

and

$$\tilde{\mathbf{p}}_{\rm sys} = \frac{e_{\rm sys}\mathbf{u}}{c^2\sqrt{1-u^2/c^2}}. \tag{69}$$

Here, the relations are simplified by taking $\mathbf{p}_{\rm sys} = 0$. Thus, the energy and the momentum carried by the particle with an arbitrary translational velocity $\mathbf{u}$ can be obtained from equations (68) and (69).

It is to be noted that we are non-committal about the mass of the charged particle throughout our formulation. The reason behind this is that there are two possible explanations for the rest mass m. The first one is in terms of the Lagrange multiplier ζ in equation (9). The second way to define m is by using the rest energy $e_{\rm sys}$. In our view, this issue cannot be resolved before understanding how the localized charge continuum reacts to an external field. As such analysis is beyond the scope of the present article for isolated systems, the resolution of the question would be a matter for future investigations.

6.3. Unsteady variations in steadily rotating system

The stationary fields in asymmetrically rotating frame reveal an inherent temporal variation when viewed by an inertial observer. It is an obvious but often ignored consequence of steady rigid body rotation about an axis which is not a line of axial symmetry. The effect is akin to an oscillating wake created by a rotating blade inside a fluid. In general, such periodic variation is always present if any asymmetrically rotating rigid body is responsible for creating spatially and temporally varying fields. In our system, electric and magnetic fields exhibit similar behavior which can be quantified by decomposing the rotation tensor $\mathbf{R}$ using discrete Fourier transform.

Any vector field $\mathbf{b}$ given by equation (29) can be decomposed in terms of complex functions

$$\mathbf{b} = \mathbf{R}\cdot\mathbf{b}_o(\mathbf{x}_o) = \mathrm{e}^{\mathrm{i}\omega t}\mathbf{b}_o^{+} + \mathrm{e}^{-\mathrm{i}\omega t}\mathbf{b}_o^{-} + \mathbf{b}_o^{0}. \tag{70}$$

The complex vector fields $\mathbf{b}_o^{\pm}$ and $\mathbf{b}_o^{0}$ are given by

$$\mathbf{b}_o^{\pm} = \mathbf{R}^{\pm}\cdot\mathbf{b}_o, \qquad \mathbf{b}_o^{0} = \mathbf{R}^{0}\cdot\mathbf{b}_o, \tag{71}$$

where temporally invariant second order tensors $\mathbf{R}^{\pm}$ and $\mathbf{R}^{0}$ are obtained by decomposing $\mathbf{R}$

$$\mathbf{R} = \mathrm{e}^{\mathrm{i}\omega t}\mathbf{R}^{+} + \mathrm{e}^{-\mathrm{i}\omega t}\mathbf{R}^{-} + \mathbf{R}^{0}. \tag{72}$$

One can derive their expressions

$$\mathbf{R}^{\pm} = (\mathbf{I} - \hat{\mathbf{e}}\hat{\mathbf{e}} \mp \mathrm{i}\mathbf{E}\cdot\hat{\mathbf{e}})/2, \qquad \mathbf{R}^{0} = \hat{\mathbf{e}}\hat{\mathbf{e}}, \tag{73}$$

in which no time-dependence is present.

Thus, if the axis of rotation is fixed with respect to the inertial observer, the predominant unsteady variation in the vector field $\mathbf{b}$ would be noticeable in the form of a periodic oscillation with frequency $\omega/(2\pi)$. Any long-range electrodynamic variable like electric field, magnetic field, Poynting vector can be represented by $\mathbf{b}$. The larger scales in the variations of these fields are embedded in the functions $\mathbf{b}_o^{\pm}$ and $\mathbf{b}_o^{0}$. These correspond to slower temporal and more gradual spatial changes compared to the predominant oscillation manifested by $\exp(\pm\mathrm{i}\omega t)$ which is recognized as small-scale behavior.

When the particle translates with a steady velocity $\mathbf{u}$ with respect to a new observer, the predominant temporal

oscillation morphs into a more complex variation dramatically. For the new observer, the time $\tilde{t}$ and the position vector $\tilde{\mathbf{r}}$ obey the rule of Lorentz transformation relating t relevant to the earlier reference frame:

$$t = \frac{\tilde{t}}{\sqrt{1 - u^2/c^2}} + \frac{\mathbf{u} \cdot \tilde{\mathbf{r}}}{c^2\sqrt{1 - u^2/c^2}}. \tag{74}$$

This reveals a new frequency and wave-number for oscillating fields to a static observer

$$\tilde{\omega} = \frac{\omega}{\sqrt{1 - u^2/c^2}}, \qquad \tilde{\boldsymbol{\lambda}} = \frac{\omega \mathbf{u}}{c^2\sqrt{1 - u^2/c^2}}. \tag{75}$$

The transformed frequency $\tilde{\omega}$ and wave-number $\tilde{\boldsymbol{\lambda}}$ are identified from variation of t in $\tilde{t}$–$\tilde{\mathbf{r}}$ space when equation (74) is substituted in the small-scale variation $\exp(\pm \mathrm{i}\omega t)$.

When ω and $\mathbf{u}$ in equations (66), (68) and (69) are expressed in terms of $\tilde{\omega}$ and $\tilde{\boldsymbol{\lambda}}$, remarkable relations can be derived

$$\tilde{e}_{\mathrm{sys}} = \frac{\mu_0 q^2 c}{4\pi\bar{\alpha}}\,\tilde{\omega}, \tag{76}$$

and

$$\tilde{\mathbf{p}}_{\mathrm{sys}} = \frac{\mu_0 q^2 c}{4\pi\bar{\alpha}}\,\tilde{\boldsymbol{\lambda}}. \tag{77}$$

These are the proportionalities similar to quantum mechanical postulates proposed by Planck and de Broglie.

If $1/\bar{\alpha}$ in equation (67) coincides with fine structure constant for an asymmetrically rotating system, the proportionality constant in equations (76) and (77) matches with reduced Planck constant. The resulting relations are true not because of any quantum mechanics postulate. On the contrary, if the particle has to maintain its integrity, it has no option but to contain energy and momentum which are proportional to the frequency and wave-number of the field variables revealed to an inertial observer.

The presented model can be related to the known phenomenon 'zitterbewegung' which suggests a cyclic motion of the particle-center superimposed to rectilinear translation. It is theorized by Schrodinger from the solution of Dirac's equation [21]. The frequency of the rigid body rotation predicted in this paper corresponds exactly to the same for zitterbewegung. Moreover, the momentum-vorticity theorem in equation (21) and subsequent field solutions indicate further connections between our analysis and the quantum description. According to our theory, a spatially variable ζ can make the centers of charge and mass different. Furthermore, our description allows many shape of the same deformable body as long as $\nabla \times \mathbf{p}$ remains the same for all possible material elements. Thus, there can be arbitrary change in the separating distance between the centroid of mass and the axis of rotation. Either way, it is possible to perceive a cyclic motion of the particulate center. In that case, details of the dynamics would be specified by the aforementioned separation and the overall translation of the entire system. This causes a decoupling between the velocity of the centroid and the net momentum stored in the electromagnetic field. If the separating distance changes, the geometry of the charge continuum also alters due to the inherent deformability of the charged continuum inside its interior. If the associated deformation field is counted as an independent variable, the phase space for the conceived dynamics matches exactly with the one proposed by Barut and Zanghi [5]. Such observations imply potential value of the outlined continuum formulation for deeper understanding of fundamental physics.

7. Summary and conclusions

This paper shows how a slightly modified interpretation of classical mechanics can explain the sustained integrity of a charged body. The key aspect of the theory is the conception of a localized continuum for the charge occupying a finite volume even if it is extremely small. Such a model requires description of the motion of an arbitrarily chosen infinitesimally small material element inside the particle. This is achieved by two classical Lagrangian principles. The only change introduced in the well-known formulation is the replacement of mass by a scalar field acting as a Lagrange multiplier for the kinematic constraint inherent in special theory of relativity.

The formulation reveals that a steady rigid body rotation can represent the velocity field inside the localized continuum with sustained integrity. This fact is congruent to the notion of inherent spin of a charged particle. Also, such observation leads to a convenient property where a functional referred as combined potential can be proven to be a constant of space. When this constancy relation is coupled with Maxwell's equations and appropriate boundary conditions, the geometry and the interior charge distribution needed for the continued coherence of the system can be determined. As a result, the electrodynamic force provides the required centripetal acceleration for circular motion, and surface integral of Poynting vector disappears making the dynamics non-dissipative. These facts are tested with simulations of slender annuli steadily rotating about their axis of symmetry.

A modified version of the same simulation can be applied for a system steadily rotating about a line which is not the axis of symmetry. In that case, an inertial observer can detect periodic spatial and temporal variations in electrodynamic fields. We have shown that the observed frequency and wave-number are directly proportional to the measured energy and momentum of the system in that reference frame, respectively. This seems to be, at least apparently, an analytical construction of Planck's and de Broglie's laws considered as quantum postulates. As the analysis also shows how to calculate the associated proportionality constant, a mathematical recipe for numerical evaluation of the fine structure constant may be derived from the presented theory.

The physical implication of the obtained results should be viewed with both excitement and caution—it is not clear yet whether the theory truly signifies new understandings or merely presents some intriguing coincidences. In one hand, it has the potential to explain fundamental dynamics of matter and motion in a new way. On the other hand, it can simply be a description which matches with a few known physical

postulates serendipitously. A true evaluation in this regard is possible only if the following three studies are successfully completed.

The first and foremost of these unresolved questions is how the described system interacts with an externally imposed field or another particle at proximity. Our present study concentrates on an isolated body which can have self-sustained coherence. As a result, it deliberately avoids the issues pertinent to external interactions. The consideration of an external field would, however, reveal whether our theoretical frame-work can reproduce quantum mechanical results like energy-levels in different bound states or spin manifestation in presence of a magnetic field. Moreover, this would show us the true measure of particulate mass which should be defined as the curvature response to an imposed force field. We can, then, extend the many-body dynamics to analyze inter-particle interactions and collisions.

The second study should investigate the stability criteria for particles under the action of an external field or perturbation. The systems described in this paper maintain self-sustaining integrity when isolated from external impetus. These can be, however, quite unstable if the dynamics is perturbed. Hence, one can hypothesize that many possible configurations permissible under our present consideration may only be partially stable or totally unstable in real world.

The third and final analysis would involve specific simulation for the domains which satisfy the stability criteria under external perturbation. This requires identification of the systems which are at least partially stable. Then, the computation of the field and the geometry associated to these particles will lead to the calculation of fine structure constant whose accurate evaluation can be viewed as the final triumph of the presented theory.

If the three proposed studies are successfully concluded, a new paradigm for elementary charged particles can be theorized. Then, one can infer the classical electrodynamics inside charged continuum with spatially varying ζ is indeed the most basic principle of mechanics in the smallest possible scale. All quantum phenomena are relatively large-scale manifestations of this fundamental dynamics quantifying many-body interactions spanned across interparticle separation much larger than particulate dimensions. Thus, processes like wave-function collapse or short-time variations during scattering should be explained by the new continuum model. In contrast, quantum mechanics should be reserved for description of the states attained long after the transiency caused by collision or sudden fluctuations. Reality of the physical world might be captured in new details by such hierarchy of multiscale theories.

Acknowledgments

The required institutional support for this work has been provided by St. Xavier's College, Kolkata, India. Also, the author is thankful to Prof David Griffiths for useful comments and suggestions on the analysis presented in the paper.

ORCID iDs

S Bhattacharya https://orcid.org/0000-0002-9205-6575

References

[1] Griffiths D 2008 *Introduction to Elementary Particles* (Weinheim: Wiley-VCH)
[2] Dirac P 1938 *Proc. R. Soc.* A **167** 148
[3] Pryce M 1938 *Proc. R. Soc.* A **168** 389
[4] Born M 1936 *Proc. R. Soc.* A **165** 291
[5] Barut A O and Zanghi N 1984 *Phys. Rev. Lett.* **52** 2009
[6] Maddox J 1987 *Nature* **325** 306
[7] Rodrigues W A, Vaz J and Recami E 1993 *Found. Phys.* **23** 459
[8] Salesi G and Recami E 1994 *Phys. Lett.* **190** 137
[9] Guralnik G S 2009 *Int. J. Mod. Phys.* A **24** 2601–27
[10] Zenczykowski P 2008 *Phys. Lett.* B **660** 567
[11] Tangherlini F 1962 *Nuovo Cimento* **26** 497
[12] Einstein A and Rosen N 1935 *Phys. Rev.* **48** 73
[13] Arnowitt R, Deser S and Misner C 1960 *Phys. Rev.* **120** 313
[14] Landau L D and Lifshitz E M 1987 *Mechanics: Course of Theoretical Physics* (New York: Pergamon)
[15] Griffiths D 1994 *Introduction to Electrodynamics* (New Jersey: Prentice Hall)
[16] Saffman P 1993 *Vortex Dynamics* (Cambridge: Cambridge University Press)
[17] Bhattacharya S 2005 *J. Fluid Mech.* **538** 291
[18] Bhattacharya S 2007 *J. Fluid Mech.* **590** 147
[19] Davidson P 1994 *J. Fluid Mech.* **276** 273
[20] Hinsen K and Felderhof B U 1992 *J. Math. Phys.* **33** 3731
[21] Schrodinger E 1930 *Sitzunger. Preuss. Akad. Wiss. Phys. Math. Kl.* **24** 418